

Crime Modeling with Truncated Lévy Flights and the Effects of Law Enforcement Actions

Chaohao Pan*, Bo Li†, Yuqi Zhang‡, Nathan Geldner§,
Chuntian Wang¶, Li Wang||, Andrea Bertozzi¶

September 21, 2016

Abstract

In this paper, we develop a statistical model of criminal behavior with the application of the truncated Lévy flights, motivated by the previous crime models applying the random walks as in [M. B. Short, M. R. D’Orsogna, V. B. Pasour, G. E. Tita, P. J. Brantingham, A. L. Bertozzi, and L. R. Chayes, *Math. Models Methods Appl. Sci.*, 18 (2008), pp. 1249-1267] and the Lévy flights as in [S. Chaturapruek, J. Breslau, D. Yazdi, T. Kolokolnikov, and S. G. McCalla, *SIAM J. Appl. Math.*, 73(4) (2013), pp. 1703–1720]. On the discrete level, we assume that each criminal travels through space independently according to a truncated Lévy flight (that is, with a limited jump range reflecting a limited traveling distance) biased towards the attractive burglary sites characterized by a dynamic attractiveness field. Thus, the models in the previous works mentioned above can be treated as special cases of our model, with the truncation size varying from a single step size to the infinity. Then based on this lattice model, we derive a continuum limit, which is in good agreement with the discrete system. We observe that a local operator arises rather than a non-local operator in the continuum system, essentially due to the fact that the generator of the truncated Lévy process is the Laplace operator. Next we incorporate the law enforcement agents into the model following the ideas in [P. A. Jones, P. J. Brantingham, and L. R. Chayes, *Math. Models Methods Appl. Sci.*, 20 (2010), pp. 1397-1423]. To compare the effects of different patrolling strategies (including an unbiased random walk, a biased random walk, and a truncated Lévy flight) quantitatively, we evaluate the total number of burglary events occurring in a given time frame and find that the truncated Lévy flight is the most effective in terms of reducing this quantity.

Keywords: Crime models; Lévy flights; continuum limit; linear stability; police patrol.

2010 *Mathematics Subject Classification* Primary: 35R60; Secondary: 35Q84.

*Center for Atmosphere Ocean Science, Courant Institute, New York University, New York, NY 10012

†Department of Mathematics, University of California, Berkeley, Berkeley, CA 94720

‡Language Technologies Institute, Carnegie Mellon University School of Computer Science, Pittsburgh, PA 15213

§Department of Mathematics, Harvey Mudd College, Claremont, CA 91711

¶Department of Mathematics, University of California, Los Angeles, Los Angeles, CA 90095

||Department of Mathematics and Computational and Data-Enabled Science and Engineering Program, State University of New York at Buffalo, Buffalo, NY 14206

Contents

1	Introduction	3
2	The Truncated Lévy Flight Model (TLFM)	4
2.1	Discrete Model	4
2.1.1	Evolution of the Attractiveness Field	4
2.1.2	Evolution of the Distribution of Criminals	5
2.2	Continuum Limit	6
2.3	Numerical Simulations	8
2.4	Linear Stability Analysis	9
2.5	Comparison with the Previous Models	10
2.5.1	Comparison between the TLFM and the RWM	10
2.5.2	Comparison between the TLFM and the LFM	11
3	Modeling the Effects of the Police Patrol	12
3.1	Effects on the Criminal Behavior and Dynamics	12
3.2	Dynamics of the Law Enforcement Agents	13
3.2.1	Random Walk	13
3.2.2	Biased Random Walk	14
3.2.3	Biased Truncated Lévy Flight	15
3.3	Evaluation of Different Patrol Strategies	16
3.4	Simulations in Two-Dimensional Space	20
4	Discussion	21
5	Appendix	22
6	Acknowledgements	23

1 Introduction

Crime modeling has been a fast growing field with impactful applications in the recent years. Specifically, the UCLA model in [29] (hereafter referred to as the “Random Walk Model (RWM)”) has helped more than thirty cities worldwide to curb crimes. Following this pioneering work, many related fields have been explored, such as modeling and simulation of gang rivalries, social networks and terrorist aggregations [1, 2, 10, 14, 15, 17, 23, 24, 25, 26, 32, 33].

The UCLA model assumes that the criminals follow a biased random walk (towards regions with high “attractiveness”), which is an underlying scalar field evolving according to the “repeat or near-repeat victimization” and “broken windows effect”. Rooted in criminology research, these concepts describe the phenomenon that a place and its neighborhood become more attractive to criminals once a crime* has occurred there [5, 29]. Previous works on criminal modeling have considered these effects as critical factors governing the evolution of the attractiveness field [5, 8, 11]. Utilizing these ideas, [29] has constructed a statistical model of criminal behavior which successfully picks up the feature of hotspots in crime dynamics, that is, regions with high crime rates [3, 27], and compares favorably with the real data [28]. However, the assumption that criminals follow a random walk with constant speed is rather restricted, as in the real life, they can travel much farther to commit a crime; in fact data of distances between homes of criminals and their targets suggest that they are willing to make long trips for valuable targets [22, 30]. Moreover in general the human movement is better modeled with Lévy flights rather than the random walks [4, 9, 12]. To this end, Chaturapruek et al. have developed in [6] a new model (which we will hereafter refer to as the “Lévy Flight Model (LFM)”), assuming that the criminals move according to a Lévy flight, that is, they can travel arbitrarily far in one time step with a probability proportional to attractiveness of the destination and inversely proportional to some power of the distance (see also [7]).

What we focus on here is to extend the Lévy Flight Model (FLM) to include a jump range limit. Indeed in real life no criminal can move arbitrarily far in a single time step. Furthermore, the movement patterns such as the mobility of different types of criminals can vary greatly, e.g. between professional criminals and amateur ones [16, 30]. With these facts in mind, we propose a “Truncated Lévy Flight Model (TLFM)” with a truncation of the Lévy flights so that arbitrarily long jumps are excluded. Modeling using the truncated Lévy flights has been applied in many areas such as finance [19, 20, 21], and it is proven that the sum of independent truncated Lévy flights converges to a Gaussian process [18]. As an analog, in the derivation of the continuum limit for our model, due to the truncation, the Laplace operator arises rather than the fractional Laplace operator for the Lévy Flight Model [6, 35]. More specifically this is because the generator of the truncated Lévy flight is local, due to the fact that the range of the truncated Lévy distribution is compact. Thus our model incorporates both the “nonlocal” feature (allowing long jumps) and the “local” feature (restricting the jump range). Moreover as mentioned above, by adjusting the size of the truncation which controls the parameters in the limit equations, we can simulate criminal dynamics of different types with different mobility. To conclude, the TLFM is an extension of the RWM (when the size of the truncation is the same as a single step size), and also an extension of the LFM, which can be approximated by the TLFM when the size of the truncation goes to infinity. These results agree with the theoretical conclusions in [18].

*As in [29] mostly we focus on residential burglaries rather than crimes in general.

For the next step, we examine the effects of the law enforcement on the TLFM, focusing on choosing a most efficient patrolling strategy (see also [13]). We adopt the same basic assumption that the attractiveness of a site that the criminals perceive decreases exponentially with the number of the patrolling agents at that site. The patrolling strategies proposed in [13] include an unbiased random walk, a biased random walk towards the sites with high attractiveness, and a “peripheral interdiction” which sends the police to perimeters (instead of the centers) of crime hotspots. However, since the criminals in the TLFM can take long jumps, protecting the perimeters of a hotspot does not necessarily prevent them from entering the center, and hence we instead propose patrolling according to a biased truncated Lévy flight. Then we compare the effects of the above strategies quantitatively by measuring the total number of crimes committed in a given time period. Simulations with various initial conditions show that the biased truncated Lévy flight is the most efficient.

The rest of the paper is organized as follows. In Section 2, we review the basic assumptions of the repeat and near-repeat victimization to construct the attractiveness field, and then derive, in both discrete and continuum settings, the biased truncated Lévy flights modeling the criminal behavior. For the continuum system, we apply a linear stability analysis to the homogeneous steady state solutions to study the formation of hotspots. Next we explore the relations and differences amongst the TLFM, the RWM and the LFM. Then in Section 3, we incorporate the law enforcement agents into the model and compare the efficiency of different patrolling strategies through simulations. Section 4 is for discussions. Finally, Section 5 includes an appendix for some details of derivations and proof.

2 The Truncated Lévy Flight Model (TLFM)

We assume that the domain is a one-dimensional grid graph[†] with grid length l and periodic boundary conditions, unless otherwise specified.

2.1 Discrete Model

We will introduce the dynamics of the local attractiveness and then the evolution of the distribution of the criminals.

2.1.1 Evolution of the Attractiveness Field

Following [6, 13, 29], we describe the varying vulnerability to burglary events of different sites by a dynamic attractiveness field. Criminals are more likely to travel to areas with higher attractiveness, and more likely to commit crimes once they are there. To describe the evolution of attractiveness over time at a site k , we decompose the attractiveness field as

$$A_k(t) = A_k^0 + B_k(t), \quad (1)$$

where A_k^0 is a static term depending only on k , and $B_k(t)$ is a dynamic term encompassing the effects of repeat and near-repeat victimization. Let $E_k(t)$ be the number of crimes committed in the time interval $(t, t + \delta t)$ at site k . Considering only the self-exciting nature of crime we can then express the evolution of $B_k(t)$ as $B_k(t + \delta t) = B_k(t)(1 - \omega\delta t) + \theta E_k(t)$, where ω is the decay rate of the attractiveness field, and θ is the increase in B_k for each

[†]The model can be easily extended to any connected graph, which accurately reflects the geometry of a city.

crime that occurs at k . If we further include the near-repeat victimization, the evolution equation of $B_k(t)$ can be expressed as

$$B_k(t + \delta t) = \left[(1 - \eta)B_k(t) + \frac{\eta}{2}(B_{k-1}(t) + B_{k+1}(t)) \right] (1 - \omega\delta t) + \theta E_k(t), \quad (2)$$

where $\eta \in (0, 1)$ is a constant measuring the significance of the near-repeat victimization effect. To specify $E_k(t)$, we make more assumptions about the criminal behaviors. Initially, a given number of criminals are distributed over the graph, whose movement is restricted to discrete time steps $t = n\delta t, n \in \mathbb{N}, \delta t > 0$. We denote the density of criminals at site k during the time interval $[t, t + \delta t)$ as $\mathbf{N}_k(t)$. Following the settings in the Random Walk Model as in [6] and [29], we assume that in $(t, t + \delta t)$, a criminal either moves to another site, or commits a crime following a standard Poisson process, whose probability, denoted as $p_k(t)$, is given by

$$p_k(t) = 1 - e^{-A_k(t)\delta t}. \quad (3)$$

This implies that the (conditional) expectation of $E_k(t)$ equals to $\delta t A_k(t) \mathbf{N}_k(t)$. Hence (2) becomes

$$B_k(t + \delta t) = \left[(1 - \eta)B_k(t) + \frac{\eta}{2}(B_{k-1}(t) + B_{k+1}(t)) \right] (1 - \omega\delta t) + \theta \delta t A_k(t) \mathbf{N}_k(t). \quad (4)$$

Remark 2.1. Here we observe that (4) is actually a formal identity, as the rigorous equality will require e.g., the independence of A_k and \mathbf{N}_k (see also [13]). However as discussed in [31], we can neglect the local correlations here, since the large-scale correlations are more important in reflecting the intrinsic nature of the system, especially when it comes to the continuum limit later.

2.1.2 Evolution of the Distribution of Criminals

In the Random Walk Model (RWM), the criminals can only move to a neighboring site in each time step. By contrast, in the Lévy Flight Model, the criminals can move to any site on the graph in one step [6]. However here we assume that one can move no more than L grid steps within one time step, where $L \in \mathbb{N}$. The relative transition likelihood, $w_{i \rightarrow k}$, is defined subject to a truncated Lévy power law

$$w_{i \rightarrow k} = \begin{cases} \frac{A_k}{l^\mu |i - k|^\mu}, & 1 \leq |i - k| \leq L, \\ 0, & \text{otherwise,} \end{cases} \quad (5)$$

where $\mu \in (1, 3)$. In other words, arbitrarily long jumps are not allowed in a truncated Lévy flight. The (normalized) transition probability is then defined as

$$q_{i \rightarrow k} = \frac{w_{i \rightarrow k}}{\sum_{j \neq i} w_{i \rightarrow j}}. \quad (6)$$

Recall that in the time interval $(t, t + \delta t)$, a criminal either commits a crime (following the standard Poisson process as in (3)) or else moves on according to the biased truncated Lévy flight defined as above. At the same time, new criminals appear with a constant rate Γ . Hence these assumptions together imply that the criminal density evolves in a single time step as follows

$$\mathbf{N}_k(t + \delta t) = \sum_{\substack{i \in \mathbb{Z} \\ 1 \leq |i - k| \leq L}} [1 - A_i(t)\delta t] \mathbf{N}_i(t) q_{i \rightarrow k}(t) + \Gamma \delta t. \quad (7)$$

Here we adopt the same kind of understanding as in Remark 2.1 of this formal identity.

2.2 Continuum Limit

Now we take the continuum limit for the above discrete model as δt and l both converge to 0. Following the same procedure as in [6] and [29], and assuming that the quantity $\theta\delta t$ remains fixed with a certain absolute constant (which, without loss of generality, we set as $\theta\delta t = 1$), we can derive the continuum limit for $A(t)$ in (4) as follows

$$A_t = \frac{l^2\eta}{2\delta t} A_{xx} - \omega(A - A^0) + \mathbf{A}\mathbf{N}\theta, \quad (8)$$

where A_t denotes $\frac{\partial A}{\partial t}$ and A_{xx} denotes $\frac{\partial^2 A}{\partial x^2}$ (the same type of notations will be adopted for partial derivatives hereafter).

The derivation of the continuum limit for \mathbf{N} , however, is more difficult, and much different from the process in [6] due to the truncation of the Lévy flight. To begin with, we define

$$z_L := 2 \sum_{k=1}^L \frac{1}{k^\mu}, \quad (9)$$

and

$$\mathcal{L}(f_i) := \sum_{\substack{j \in \mathbb{Z} \\ 1 \leq |i-j| \leq L}} \frac{f_j - f_i}{(|j-i|l)^\mu}. \quad (10)$$

Then it follows immediately from (5) that

$$\sum_{\substack{i \in \mathbb{Z} \\ 1 \leq |i-k| \leq L}} w_{i \rightarrow k} = l^{-\mu} z_L A_i + \mathcal{L}(A_i). \quad (11)$$

With (11) and (6), we obtain

$$\begin{aligned} q_{i \rightarrow k} &= \frac{w_{i \rightarrow k}}{\sum_{\substack{j \in \mathbb{Z} \\ 1 \leq |j-k| \leq L}} w_{i \rightarrow j}} = \frac{w_{i \rightarrow k}}{l^{-\mu} z_L A_i \left(\frac{\mathcal{L}(A_i)}{l^{-\mu} z_L A_i} + 1 \right)} \\ &\sim w_{i \rightarrow k} \left[\frac{1}{l^{-\mu} z_L A_i} - \frac{\mathcal{L}(A_i)}{(l^{-\mu} z_L A_i)^2} \right] \\ &= \frac{A_k}{|i-k|^\mu} \left(\frac{1}{z_L A_i} - \frac{\mathcal{L}(A_i) l^\mu}{A_i^2 z_L^2} \right), \quad 1 \leq |i-k| \leq L, \end{aligned} \quad (12)$$

where, in the second step, we have applied the approximation $\frac{1}{1+x} \sim 1 - x$ for small x . We then obtain by (7)

$$\frac{\mathbf{N}_k(t + \delta t) - \mathbf{N}_k(t)}{\delta t} = \frac{1}{\delta t} \left[\sum_{1 \leq |i-k| \leq L} \mathbf{N}_i (1 - A_i \delta t) q_{i \rightarrow k} - \mathbf{N}_k \right] + \Gamma. \quad (13)$$

Now applying (12) to the RHS of (13), we obtain

$$\begin{aligned}
\frac{\mathbf{N}_k(t + \delta t) - \mathbf{N}_k(t)}{\delta t} &= \frac{1}{\delta t} \sum_{1 \leq |i-k| \leq L} \mathbf{N}_i (1 - A_i \delta t) \frac{A_k}{|i-k|^\mu} \left(\frac{1}{z_L A_i} - \frac{\mathcal{L}(A_i) l^\mu}{A_i^2 z_L^2} \right) - \frac{\mathbf{N}_k}{\delta t} + \Gamma \\
&= \frac{A_k}{\delta t} \left[\sum_{1 \leq |i-k| \leq L} (1 - A_i \delta t) \frac{\mathbf{N}_i}{A_i} \frac{1}{z_L |i-k|^\mu} - \frac{\mathbf{N}_k}{A_k} \right] \\
&\quad - \frac{A_k}{\delta t} \sum_{1 \leq |i-k| \leq L} \left[(1 - A_i \delta t) \frac{\mathbf{N}_i}{|i-k|^\mu} \frac{\mathcal{L}(A_i) l^\mu}{A_i^2 z_L^2} \right] + \Gamma. \tag{14}
\end{aligned}$$

In order to simplify (14) further, we observe that (9) and (10) implies

$$\sum_{\substack{i \in \mathbb{Z} \\ 1 \leq |i-k| \leq L}} \frac{\mathbf{N}_i}{|i-k|^\mu} = \sum_{\substack{i \in \mathbb{Z} \\ 1 \leq |i-k| \leq L}} \frac{\mathbf{N}_i - \mathbf{N}_k}{|i-k|^\mu} + \sum_{\substack{i \in \mathbb{Z} \\ 1 \leq |i-k| \leq L}} \frac{\mathbf{N}_k}{|i-k|^\mu} = l^\mu \mathcal{L}(\mathbf{N}_k) + z_L \mathbf{N}_k \sim z_L \mathbf{N}_k,$$

where we have ignored the $O(l^\mu)$ term in the final step. Hence this together with (14) implies that

$$\begin{aligned}
\frac{\mathbf{N}_k(t + \delta t) - \mathbf{N}_k(t)}{\delta t} &= \frac{A_k}{\delta t} \sum_{1 \leq |i-k| \leq L} \left[\frac{\mathbf{N}_i}{A_i} \frac{1}{z_L |i-k|^\mu} - \delta t \frac{\mathbf{N}_i}{|i-k|^\mu z_L} - \frac{\mathbf{N}_k}{A_k} \frac{1}{z_L |i-k|^\mu} \right] \\
&\quad - \frac{A_k}{\delta t} \sum_{1 \leq |i-k| \leq L} \left[\frac{\mathbf{N}_i}{|i-k|^\mu} \frac{\mathcal{L}(A_i) l^\mu}{A_i^2 z_L^2} - \frac{\mathbf{N}_i \mathcal{L} A_i}{A_i z_L^2 |i-k|^\mu} l^\mu \delta t \right] + \Gamma \\
&\sim \frac{A_k}{\delta t} \sum_{1 \leq |i-k| \leq L} \left[\frac{\frac{\mathbf{N}_i}{A_i} - \frac{\mathbf{N}_k}{A_k}}{|i-k|^\mu z_L} - \frac{\mathbf{N}_i}{|i-k|^\mu} \frac{\mathcal{L}(A_i) l^\mu}{A_i^2 z_L^2} - \delta t \frac{\mathbf{N}_i}{|i-k|^\mu z_L} \right] + \Gamma \\
&\sim \frac{l^\mu}{z_L \delta t} \left[A_k \mathcal{L} \left(\frac{\mathbf{N}_k}{A_k} \right) - \frac{\mathbf{N}_k \mathcal{L}(A_k)}{A_k} \right] - A_k \mathbf{N}_k + \Gamma, \tag{15}
\end{aligned}$$

where, at the second step, we have ignored the $O(l^\mu \delta t)$ terms in the summation. We also observe that

$$\mathcal{L}(A_k) = \sum_{\substack{j \in \mathbb{Z} \\ 1 \leq |j-k| \leq L}} \frac{A_j - A_k}{(|j-k|l)^\mu} = \frac{1}{l} \sum_{\substack{j \in \mathbb{Z} \\ 1 \leq |j-k| \leq L}} \frac{A_j - A_k}{(|j-k|l)^\mu} l \sim \frac{1}{l} \int_{I_x} \frac{A(y) - A(x)}{|y-x|^\mu} dy, \tag{16}$$

where

$$x = kl, \quad y_j = jl, \quad A_j = A(y_j), \quad A_k = A(x),$$

and for each fixed x ,

$$I_x := \left[x - (L + \frac{1}{2})l, x - \frac{1}{2}l \right] \cup \left[x + \frac{1}{2}l, x + (L + \frac{1}{2})l \right]. \tag{17}$$

Since the length of I_x is Ll , then as l converges to 0, the integration in the right hand side

of (16) is local³ at x , and we can apply Taylor expansion at x on the integrand to obtain

$$\begin{aligned}
\mathcal{L}(A_k) &= \frac{1}{l} \int_{I_x} |y-x|^{-\mu} \left[A_x(x)(y-x) + A_{xx}(x) \frac{(y-x)^2}{2} + O((y-x)^3) \right] dy \\
&\sim \frac{1}{l} \left[\int_{I_x} \frac{A_x(x)(y-x)}{|y-x|^\mu} dy + \int_{I_x} \frac{A_{xx}(x)(y-x)^2}{2|y-x|^\mu} dy \right] \\
&= \frac{1}{l} \int_{x+\frac{1}{2}l}^{x+(L+\frac{1}{2})l} |y-x|^{2-\mu} A_{xx}(x) dy \\
&= \frac{l^{2-\mu}}{3-\mu} \left[(L+\frac{1}{2})^{3-\mu} - (\frac{1}{2})^{3-\mu} \right] A_{xx}(x),
\end{aligned} \tag{18}$$

where, at the second step, we have ignored the $O((y-x)^{3-\mu})$ terms, since $|y-x| = O(l)$ and $\mu < 3$. Applying (18) to (15), we obtain

$$\mathbf{N}_t = \frac{l^2}{\delta t z_L (3-\mu)} \left[(L+\frac{1}{2})^{3-\mu} - (\frac{1}{2})^{3-\mu} \right] \left[A(\frac{\mathbf{N}}{A})_{xx} - \frac{\mathbf{N}}{A} A_{xx} \right] - \mathbf{A} \mathbf{N} + \Gamma. \tag{19}$$

Hence in the approximation we can choose the scaling to be $\frac{l^2}{\delta t}$ remaining an absolute constant⁴, which, without loss of generality, can be set as $1/\omega$. To simplify the expressions, we reparametrize (19) as follows

$$A = A^* \omega, \quad \mathbf{N} = \frac{\rho \omega}{\theta}, \quad t = \frac{t^*}{\omega}, \quad \eta^* = \frac{l^2 \eta}{2\omega \delta t}. \tag{20}$$

This together with (8) and (19) implies (omitting the $*$'s)

$$A_t = \eta A_{xx} - A + \alpha + A\rho, \tag{21}$$

$$\rho_t = D \left[A(\frac{\rho}{A})_{xx} - \frac{\rho}{A} A_{xx} \right] - A\rho + \beta, \tag{22}$$

where we have set

$$D = \frac{l^2}{\omega \delta t z_L (3-\mu)} \left[(L+\frac{1}{2})^{3-\mu} - (\frac{1}{2})^{3-\mu} \right], \quad \alpha = \frac{A^0}{\omega}, \quad \beta = \frac{\Gamma \theta}{\omega^2}. \tag{23}$$

Remark 2.2. In fact ρ introduced in (20) means exactly the criminal density, as $\rho = \mathbf{N}\theta\omega = \mathbf{N}/\ell^2$ given that $\theta\delta t = 1$.

2.3 Numerical Simulations

To verify the derivation of the continuum limit, we compare the discrete model (4) and (7), and the continuum limit (21) and (22) numerically. For the discrete model, we assume the grid points as x_i , $i = 1, 2, \dots, 60$, with $x_i - x_{i-1} = 1/60$. For the continuum system we consider the computational domain $x \in [0, 1]$ with $\Delta x = 1/60$, $\Delta t = 1/3600$. We use forward Euler method for the temporal discretization and spectral method for the spatial discretization. Periodic boundary conditions are implemented in both cases.

³Note that this is the essential reason that the operator we obtain is local, i.e. the Laplace operator Δ , rather than the non-local operator $\Delta^{\frac{\mu-1}{2}}$, $1 < \mu < 3$.

⁴It is unnecessary to choose the fractional-Laplace scaling as in [6], letting $\frac{l^{\mu-1}}{\delta t}$ remain a constant, $1 < \mu < 3$, since the $\frac{l^2}{\delta t}$ scaling is in consistent with the scaling for (8).

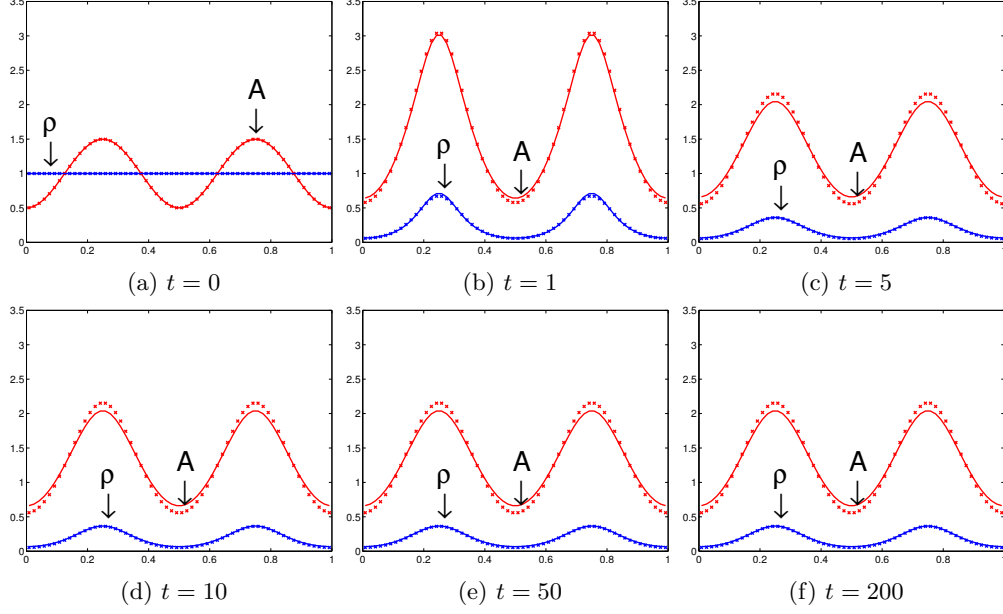


Figure 1: Simulations of the biased truncated Lévy flights when $\mu = 2.5$, $l = 1/60$, $\delta t = 0.01$, $L = 9$, $\eta = 0.1$, $\Gamma = 0.3$, and $\omega = 1$. The solid curve represents the continuum limit, and the dots represent the discrete model. The initial conditions are $A^0 = 1 - 0.5 \cos(4\pi x)$ and $\rho = 1$.

Figure 1 shows a comparison between our numerical simulations for the discrete and continuum models. Figure 2 compares the steady states of our model for different values of L , and Figure 3 compares the steady states for different values of μ . In all the figures, we can observe a fairly good agreement all the way to the boundary, for a wide range of values of L and μ . Also both systems reach a steady state with two hotspots eventually.

2.4 Linear Stability Analysis

To analyze the long-term behavior of the model, we perform a linear Turing stability analysis on (21) and (22) around the homogeneous steady state $(\bar{A}, \bar{\rho})$,

$$\bar{A} = \alpha + \beta, \quad \bar{\rho} = \frac{\beta}{\alpha + \beta}. \quad (24)$$

We perturb the steady state as follows

$$A(x, t) = \bar{A} + \delta_A e^{\lambda t} e^{ikx}, \quad \rho(x, t) = \bar{\rho} + \delta_\rho e^{\lambda t} e^{ikx}. \quad (25)$$

Substituting (25) into (21) and (22), we obtain

$$\begin{bmatrix} -\eta|k|^2 - 1 + \bar{\rho} & \bar{A} \\ \frac{2\bar{\rho}}{\bar{A}} D|k|^2 - \bar{\rho} & -D|k|^2 - \bar{A} \end{bmatrix} \begin{bmatrix} \delta_A \\ \delta_\rho \end{bmatrix} = \sigma \begin{bmatrix} \delta_A \\ \delta_\rho \end{bmatrix}, \quad (26)$$

whose detailed derivations can be found in the Appendix. Furthermore, by analyzing (26), we obtain the following theorem characterizing the necessary and sufficient conditions for the system to be unstable around the homogeneous steady state.

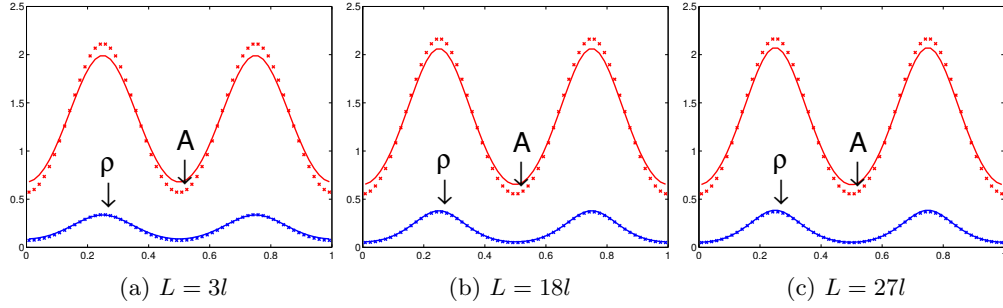


Figure 2: Comparisons of the steady state with different values of L . All the parameters are the same as in Figure 1 except for L . The shots are taken at $t = 200$.

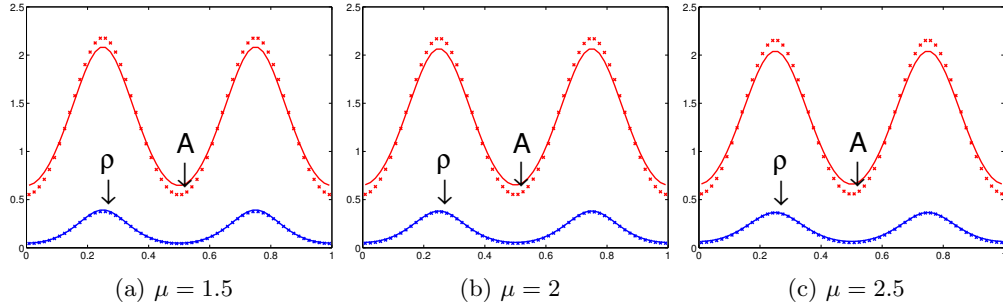


Figure 3: Comparisons of the steady state obtained with different values of μ . All the other parameters are the same as in Figure 1 except for μ . The shots are taken at $t = 200$.

Theorem 2.1. *When $\bar{\rho} < 1/3$, the homogeneous equilibrium in (24) is stable. When $\bar{\rho} > 1/3$, then the equilibrium is unstable if and only if $\bar{A} < \bar{A}_*$, where*

$$\bar{A}_* = D\eta^{-1}(\sqrt{3\bar{\rho}} - 1)^2. \quad (27)$$

A proof of Theorem 2.1 can be found in the Appendix.

2.5 Comparison with the Previous Models

Now we compare the Truncated Lévy Flight Model with the previous models, the Random Walk Model (RWM) in [29] and the Lévy Flight Model (LFM) in [6]. We note first that the limit equations for the attractiveness field are the same for all the three models, so we will focus on the differences lie in the limit equations for the density of criminals.

2.5.1 Comparison between the TLFM and the RWM

We recall the continuum limit in [29] for the criminal density in the one-dimensional Random Walk Model as follows:

$$\rho_t = D_1 \left[A \left(\frac{\rho}{A} \right)_{xx} - \frac{\rho}{A} A_{xx} \right] - A\rho + \beta, \quad (28)$$

where

$$D_1 = \frac{l^2}{2\omega\delta t}. \quad (29)$$

Hence (22) and (28) only differ in the parameters D and D_1 . As is shown in Figure 4, on the one hand, when L increases, the distance between D and D_1 also increases; on the other hand, when $L = 1$, D is very close to D_1 (which one can in fact explicitly compute). The latter case is fully expected, as $L = 1$ means that the criminals can move at most one grid in a single time step, which is exactly the same as the discrete Random Walk Model. Thus, the RWM can be considered as a special case of the TLFM when $L = 1$.

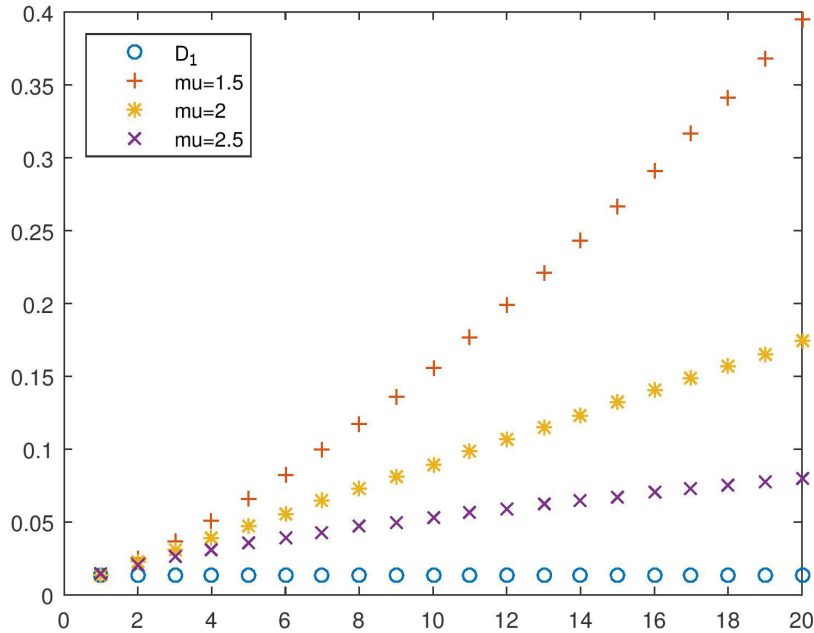


Figure 4: Comparisons of D in (23) and D_1 in (29) as a function of L with different μ 's. The other parameters are the same as those in Figure 1.

2.5.2 Comparison between the TLFM and the LFM

The continuum limit in [6] for the criminal density in the one-dimensional Lévy Flight Model is

$$\rho_t = D_2 \left[A \Delta^s \frac{\rho}{A} - \frac{\rho}{A} \Delta^s A \right] - A\rho + \beta, \quad (30)$$

where

$$D_2 = \frac{l^{2s}}{\delta t} \frac{\pi^{1/2} 2^{-2s} |\Gamma(-s)|}{z \Gamma(s + \frac{1}{2}) \omega}, \quad s = \frac{\mu - 1}{2}, \quad z = 2 \sum_{n=1}^{\infty} \frac{1}{n^\mu}.$$

Comparing (22) and (30), we observe that the difference lies in the local and non-local operators (the Laplace operator and the fractional Laplace operator respectively). At the

same time as L increases, the solution to (22) approximates the solution to (30) as is shown in Figure 5.

Furthermore, from Figure 5 we also observe that the criminals in the LFM and the TLFM are more concentrated around the hotspots than in the RWM, since the longer jumps in the Lévy flights allow criminals to aggregate on a hotspot more quickly.

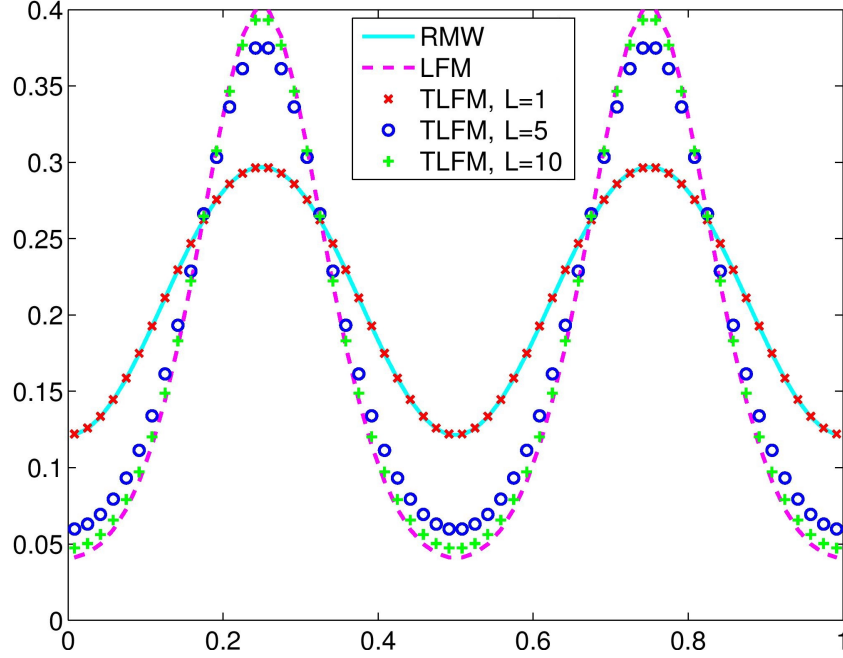


Figure 5: Comparing the evolution of the criminal density in the continuum limit of the TLFM (with jump range limit $L = 1, 5$, and 10), the RWM, and the LFM when $t = 10$. The other parameters and initial conditions are the same as in Figure 1.

3 Modeling the Effects of the Police Patrol

Following [13] where The Random Walk Model has been generalized to incorporate the effects of law enforcement actions, we consider the same extension of our model.

3.1 Effects on the Criminal Behavior and Dynamics

Let $\psi_k(t)$ be the number of officers at site k at time t . As in [13], we introduce a new variable, $\tilde{A}_k(t)$, representing the attractiveness perceived by the criminals in the presence of the police:

$$\tilde{A}_k(t) := e^{-\chi\psi_k(t)} A_k(t), \quad (31)$$

where χ is a given constant measuring the patrolling efficiency. In the discrete model, the relative transition likelihood of a criminal moving from i to k becomes

$$w_{i \rightarrow k} = \begin{cases} \frac{\tilde{A}_k}{l^\mu |i-k|^\mu}, & 1 \leq |i-k| \leq L, \\ 0, & \text{otherwise.} \end{cases} \quad (32)$$

Also a criminal commits a crime in the time interval $(t, t + \delta t)$ at site k with the probability

$$\tilde{p}_k(t) = 1 - e^{-\tilde{A}_k(t)\delta t}. \quad (33)$$

Thus, following the same reasoning as in (7) we have

$$\mathbf{N}_k(t + \delta t) = \sum_{1 \leq |i-k| \leq L} \mathbf{N}_i(1 - \tilde{A}_i\delta t)q_{i \rightarrow k} + \Gamma\delta t. \quad (34)$$

The evolution of $B_k(t)$ in (4) becomes

$$B_k(t + \delta t) = \left[(1 - \eta)B_k(t) + \frac{\eta}{2}(B_{k-1} + B_{k+1}) \right] (1 - \omega\delta t) + \delta t \tilde{A}_k \mathbf{N}_k \theta. \quad (35)$$

We observe that (34) and (35) are exactly the same as (4) and (7) except for A being substituted into \tilde{A} . Hence with the same derivations as in Section 2.2 applying the same space-time scaling, and with the same renormalization as in (20) and including $\tilde{A} = \tilde{A}^*\omega$, we obtain (omitting the *'s)

$$A_t = \eta A_{xx} - A + \alpha + \tilde{A}\rho, \quad (36)$$

$$\rho_t = D \left[\tilde{A} \left(\frac{\rho}{\tilde{A}} \right)_{xx} - \frac{\rho}{\tilde{A}} \tilde{A}_{xx} \right] - \tilde{A}\rho + \beta, \quad (37)$$

where the parameters D , α and β are defined in the same way as in (23). We note that in this model, the patrolling agents never arrest criminals but reduces the total number of burglary events by affecting the environment, that is, by affecting the attractiveness field A . We will discuss this effect in detail in the next section.

Remark 3.1. *As in Remark 2.2, here ρ is in fact the density of the criminals.*

3.2 Dynamics of the Law Enforcement Agents

We assume that the total number of the patrolling agents is a constant, reflecting the reality of limited resources. We will propose three patrolling strategies and compare their effectiveness quantitatively.

3.2.1 Random Walk

An unbiased random walk is perhaps the simplest strategy to implement. In each step, a police officer either moves one step to the left or to the right with equal probability. Thus, the evolution of the expected number of officers at site k satisfies the following relation:

$$\psi_k(t + \delta t) = \frac{1}{2} (\psi_{k-1}(t) + \psi_{k+1}(t)). \quad (38)$$

Taking the limit as l and δt both converge to 0 for the above equation, we obtain

$$\psi_t = \frac{l^2}{2\delta t} \psi_{xx}, \quad (39)$$

which is the master equation for a Brownian motion. A disadvantage of the random walk strategy is then clear: the spacial distribution of police will become nearly uniform in the long run, and hence does not give enough protection to vulnerable locations.

Figure 6 shows the effect of the unbiased random walk as a patrolling strategy. We observe that this strategy does not reduce hotspot activity, which is in consistent with the empirical evidences in [13].

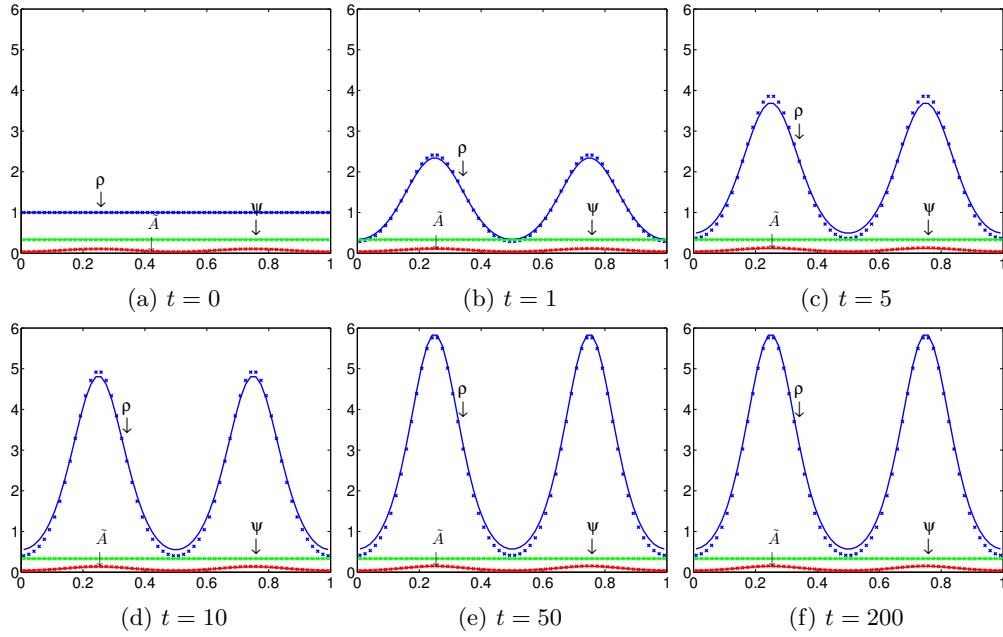


Figure 6: The comparison of the discrete model and its continuum limit when the criminals perform a truncated Lévy flight and the police perform an unbiased random walk. The green curves and dots represent the number of officers in the continuum and discrete model respectively. The parameters are the same as in Figure 1. The initial conditions for the police are $\psi = 1/3$. Also we set $\chi = 8$.

3.2.2 Biased Random Walk

In view of the disadvantage of the unbiased random walk strategy, we consider another one, biased towards the attractive sites. The discrete evolution equation for the police at site k can be written as

$$\psi_k(t + \delta t) = \frac{A_k}{A_k + A_{k-2}} \psi_{k-1}(t) + \frac{A_k}{A_k + A_{k+2}} \psi_{k+1}(t). \quad (40)$$

The corresponding continuum limit is

$$\psi_t = \frac{l^2}{2\delta t} \left[A \left(\frac{\psi}{A} \right)_{xx} - \frac{\psi}{A} A_{xx} \right]. \quad (41)$$

This strategy is also studied in [34], referred to as “cops on the dots”.

The effect of this strategy is shown in Figure 7. We observe that the long-term distribution of the police officers generally corresponds to that of the attractiveness field. Also, in average, the criminal density is lower and comes to a steady state faster than in the previous case depicted in Figure 6.

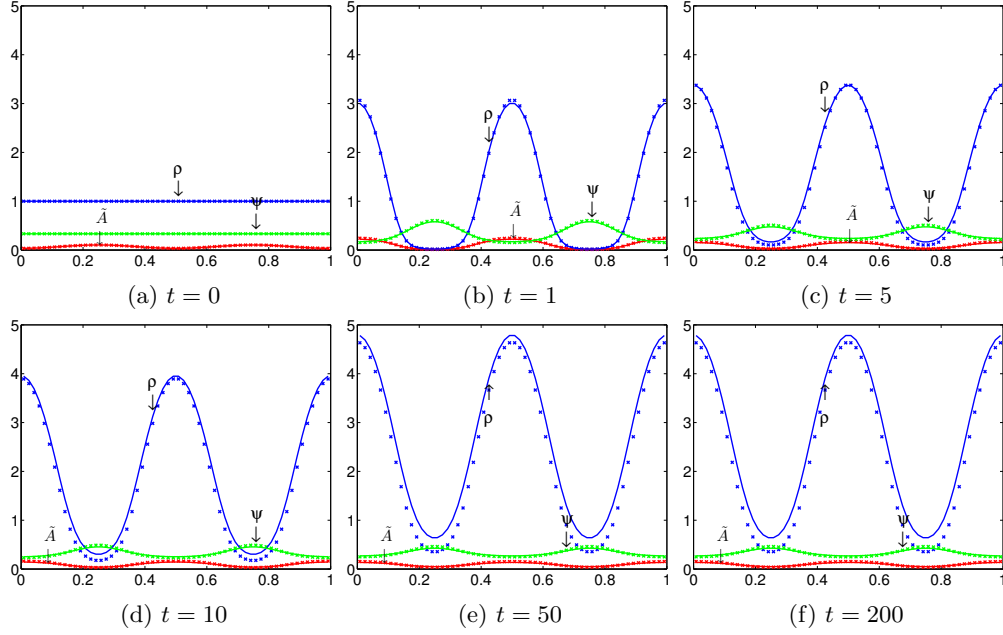


Figure 7: The comparison of the discrete model and its continuum limit when the criminals perform a truncated Lévy flight and the police perform a biased random walk. The parameters are the same as in Figure 6.

3.2.3 Biased Truncated Lévy Flight

The discrete dynamics of the police performing a biased truncated Lévy flight is as follows

$$\psi_k(t + \delta t) = \sum_{|i-k| \leq L} \psi_i(t) q_{i \rightarrow k}(t), \quad (42)$$

where

$$q_{i \rightarrow k} = \frac{w_{i \rightarrow k}}{\sum_j w_{i \rightarrow j}}, \quad (43)$$

and

$$w_{i \rightarrow k} = \begin{cases} \frac{A_k}{l^\mu |i-k|^\mu}, & 1 \leq |i-k| \leq L, \\ 0, & \text{otherwise.} \end{cases} \quad (44)$$

Here we assume that the police share with the criminals the same parameters μ and L in the underlying Lévy power law, reflecting the reality that all the kinds of transportation available to criminals are also available to the police.

In the same way as in Section 2.3, we can derive the continuum limit of the above discrete model⁵ as follows

$$\psi_t = D \left[A \left(\frac{\psi}{A} \right)_{xx} - \frac{\psi}{A} A_{xx} \right]. \quad (45)$$

Comparing the simulation results of (45) in Figure 8 with Figure 7, we see that there is not much qualitative difference between the steady states. Hence we will resort to quantitative comparisons of the models in the next section.

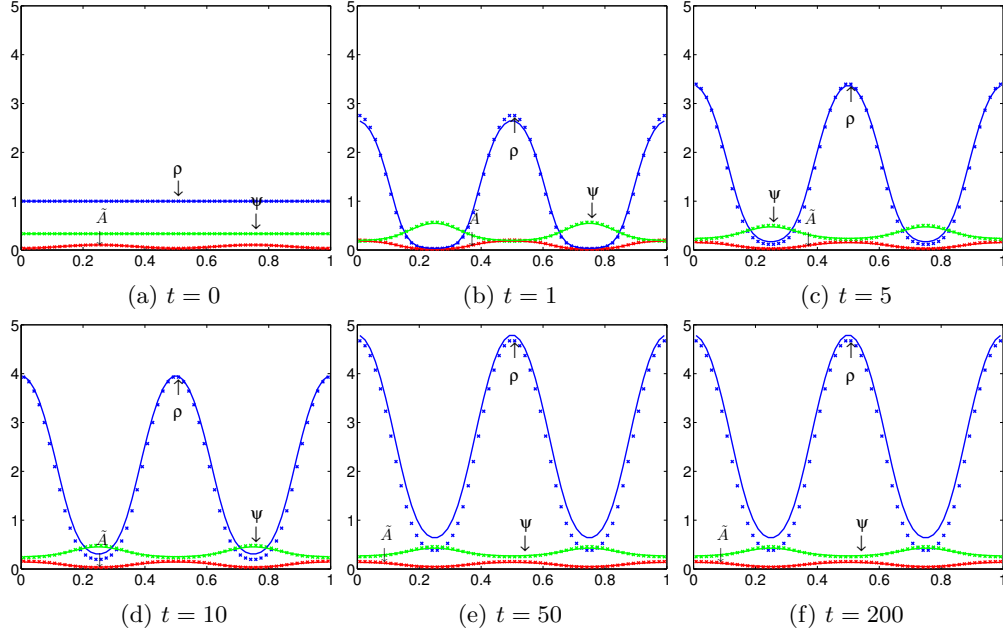


Figure 8: The comparison of the discrete model and its continuum limit when the criminals and the police both perform a biased truncated Lévy flight. The parameters are the same as in Figure 6.

3.3 Evaluation of Different Patrol Strategies

In this section, we will evaluate and compare the effectiveness of each patrolling strategy quantitatively, choosing the expectation of the density of burglary events at time t as a measure. Recall that the expected number of burglary events at location k in the time interval $(t, t + \delta t)$ equals to $\bar{A}_k(t) \mathbf{N}_k(t) \delta t$, hence the density of burglary events equals to $\bar{A}_k(t) \rho_k(t) \delta t$ (as explained in Remark 3.1). Then the total number of burglary events over the whole domain until time T has expectation $\sum_k \sum_{t < T} \bar{A}_k(t) \rho_k(t) \ell^2 \delta t$. Taking the limit

⁵We note that there is no linear terms in (45) exactly because the number of the patrolling agents is conserved.

of this double sum as t and l converge to 0, we obtain a double integral

$$\int_0^T \int_{\mathcal{M}} \tilde{A}(x, t) \rho(x, t) dx dt := S(T). \quad (46)$$

Here \mathcal{M} denotes the spacial domain. Furthermore, we define the instantaneous crime rate $R(t)$ at time t as

$$R(t) := \frac{\partial S}{\partial t}(t) = \int_{\mathcal{M}} \tilde{A}(x, t) \rho(x, t) dx. \quad (47)$$

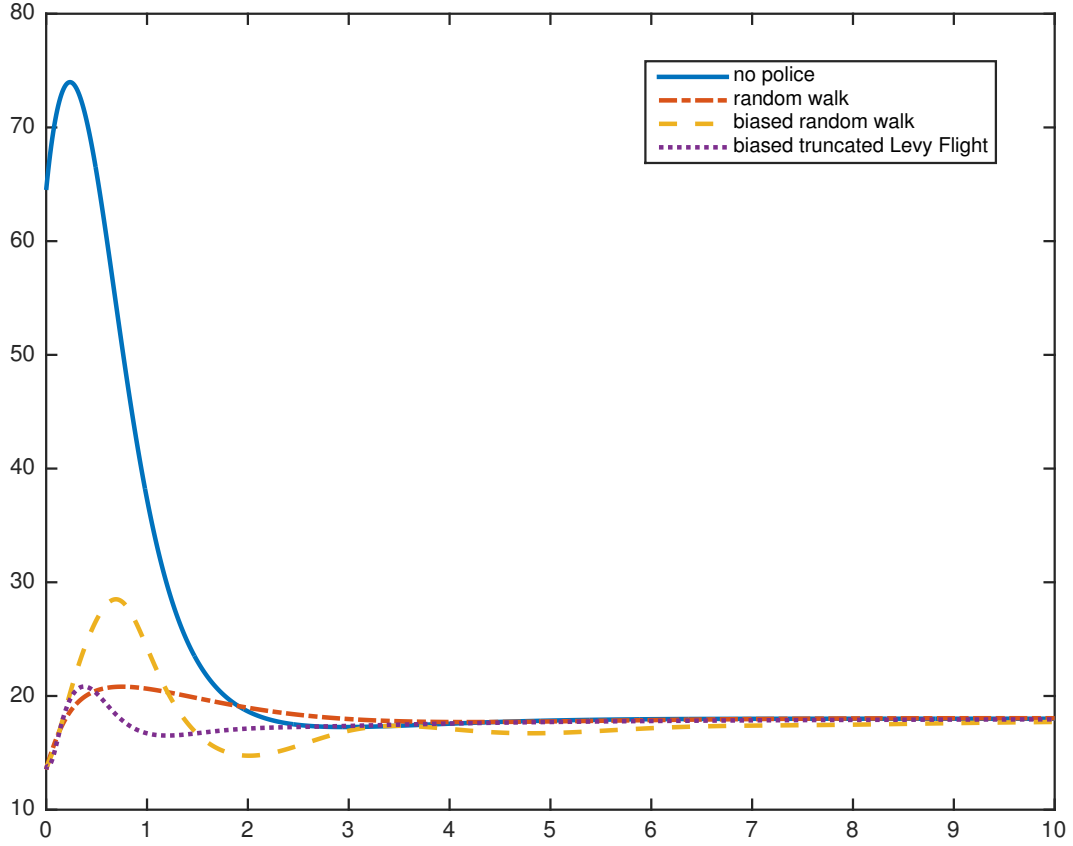


Figure 9: The plot of $R(t)$. The parameters are the same as in Figure 5. The initial conditions are $A^0 = 1 - 0.5 \cos(4\pi x)$, $\rho = 1 - 0.3 \cos(4\pi x)$, and $\psi = 1/3 \sin(\pi x)$.

Steady State of Crime Rate We observe that, the crime rate in our model, regardless of hotspot activity, will approach a constant depending only on the rate of criminals entering the system.

Theorem 3.1. *For (36) and (37) we assume the periodic boundary condition on the spacial domain \mathcal{M} . If the system of (36) and (37) is in a steady state, then the crime rate $R(t) = \beta|\mathcal{M}|$, where $|\mathcal{M}|$ is the measure of the domain \mathcal{M} .*

Proof. We integrate (37) over the domain \mathcal{M} , and obtain

$$\begin{aligned} \frac{d}{dt} \int_{\mathcal{M}} \rho &= \int_{\mathcal{M}} \rho_t = \int_{\mathcal{M}} D \left[\tilde{A} \left(\frac{\rho}{\tilde{A}} \right)_{xx} - \frac{\rho}{\tilde{A}} \tilde{A}_{xx} \right] - \tilde{A} \rho + \beta dx \\ &= \left[\tilde{A} \left(\frac{\rho}{\tilde{A}} \right)_x - \frac{\rho}{\tilde{A}} \tilde{A}_x \right] \Big|_{\mathcal{M}} - \int_{\mathcal{M}} (\tilde{A} \rho - \beta) dx. \end{aligned} \quad (48)$$

With periodic boundary conditions on \mathcal{M} , we have

$$\frac{d}{dt} \int_{\mathcal{M}} \rho = \beta|\mathcal{M}| - \int_{\mathcal{M}} \tilde{A} \rho = \beta|\mathcal{M}| - R. \quad (49)$$

When the system is at a steady state, we have

$$\frac{d}{dt} \int_{\mathcal{M}} \rho = 0.$$

It follows that

$$R(t) = \beta|\mathcal{M}|, \quad (50)$$

as desired \square

This result implies that the crime rate will eventually converge to a constant as indicated in Figure 9. Therefore, we shall only focus on the effect of police patrol before the crime rate gets too close to this constant rate. Furthermore, as is shown in Figure 9, and observed as well in other cases with different initial conditions and parameters (Table 1, 2, and 3), the crime rate is always within 5% difference compared with the steady state crime rate when $T \geq 5$. In other words, significant difference of crime rates only arise within the time interval $T \in [0, 5)$. Therefore, it is sufficient to compare $S(5)$ of different strategies as a measure of the efficiency. From Table 1, 2 and 3, we can conclude that the biased truncated Lévy flight reduces the total number of crime events most effectively as a patrolling strategy.

Police Patrol Pattern	S(5)	Improvement I	Improvement II
No Police	13874	-	-
Random Walk	9316.6	32.85%	-
Biased Random Walk	9124.6	34.23%	2.06%
Biased Truncated Lévy Flight	8750.0	36.93%	18.16%

Table 1: The expectation of the total number of burglary events before time $T = 5$ for three patrolling strategies. The parameters and initial conditions are the same as in Figure 5. ‘Improvement I’ shows the corresponding improvement compared to the situation with no police, and ‘improvement II’ represents the situation when the police perform an unbiased random walk. In this case there are two major regions of high attractiveness initially.

Police Patrol Pattern	S(5)	Improvement I	Improvement II
No Police	13827	-	-
Random Walk	9890.1	28.47%	-
Biased Random Walk	9269.0	32.96%	6.28%
Biased Truncated Lévy Flight	8836.8.0	36.09%	10.65%

Table 2: The expectation of the total number of burglary events before time $T = 5$ when the police choose different strategies. The parameters are the same as in Table 1, except that $A^0 = 1 - 0.5 \cos(8\pi x)$, and $\rho = 1 - 0.3 \cos(8\pi x)$. In this case, there are initially four regions of high attractiveness.

Police Pattern	S(5)	Improvement I	Improvement II
No Police	13758	-	-
Random Walk	10006	27.27%	-
Biased Random Walk	9227.1	32.93%	7.78%
Biased Truncated Lévy Flight	8489.5	38.29%	15.16%

Table 3: The expectation of the total number of burglary events before time $T = 5$ when the police follow different strategies. The parameters are the same as in Table 1, except that $A^0 = 1 - 0.5 \cos(16\pi x)$, and $\rho = 1 - 0.3 \cos(16\pi x)$. In this case, there are initially eight regions of high attractiveness.

3.4 Simulations in Two-Dimensional Space

In order to get a better understanding of the real life phenomena, we now simulate the discrete TLFM in the two-dimensional domain. We discretize the domain into grids, and define the distance between two grid points as their Euclidean distance. Then, we create dynamics arrays cr_{pos} and pol_{pos} to store the locations of criminals and the police. In addition, we create arrays A, B, ψ to represent A, B , and the density of the police, and 2D arrays A_{2D}, B_{2D} to represent A and B in the two-dimensional space. Furthermore, we represent the number of crimes committed at each spot at each time step by the array E . At each time step a specific agent (a criminal or a police officer) will make his or her own decision based on the assumptions of the discrete model as in Section 3. The outline of the algorithm is as follows.

Program 2D Simulation

```

input  $n, \Delta t$  number of criminals  $N_c$ , number of the police  $N_p$ , initial attractiveness  $A_0(x_i)$ , and model parameters  $L, \mu, \eta, \omega, \beta, \chi$ 

for  $t_k = 1 : (t/\delta t)$ 
    Initialize  $E$  to be 0.
    Calculate the probability of a criminal committing a crime at each spot.
    for  $i = 1 : N_c$ 
        Determine whether the  $i^{th}$  criminal will commit a crime based on its location and a random number we generate.
        If it commits a crime, update  $E$ .
        Otherwise, determine where it goes following a biased truncated Lévy flight.
        Update  $cr_{pos}$ .
    end
    for  $i = 1 : N_p$ 
        Determine where the  $i^{th}$  patrolling agent will go based on the strategy of the police.
        Update  $pol_{pos}$ .
    end
    Update  $\psi$  based on  $pol_{pos}$ .
    Update  $A, B$  based on  $E$  and  $\psi$ .
end
end 2D Simulation

```

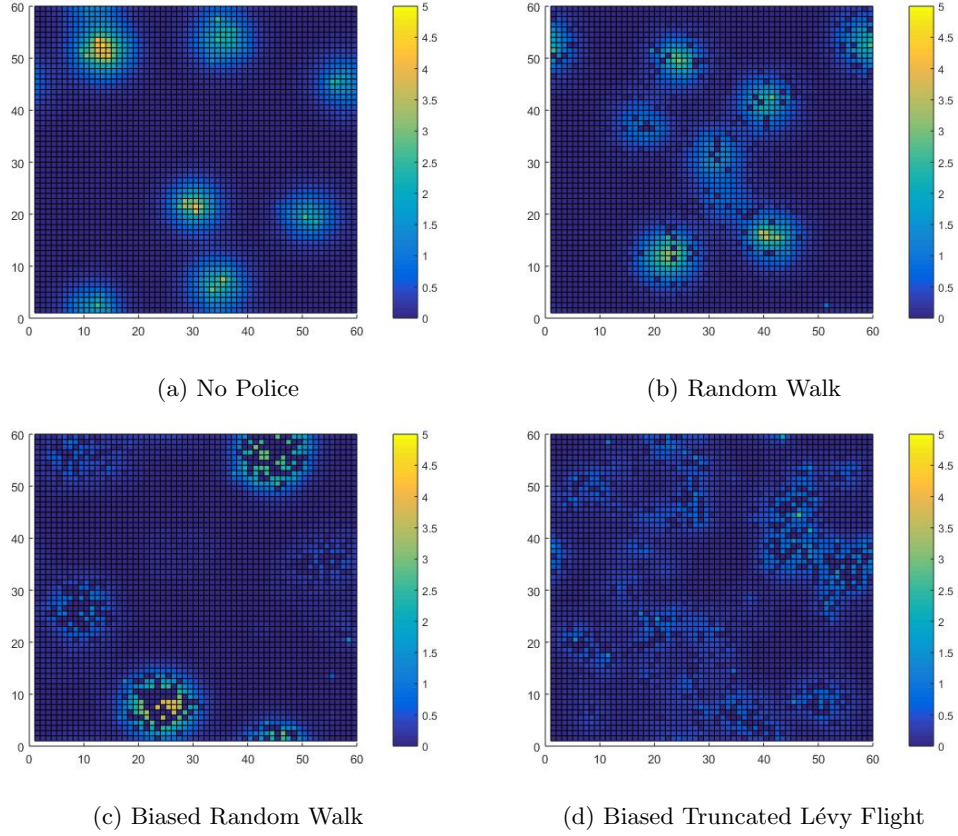


Figure 10: The simulations in two dimension when the police follow different patrolling strategies. The color represents the value of the attractiveness. We set $\mu = 2.5$, $l = 1/60$, $\delta t = 0.01$, $L = 9$, $\omega = 1/15$, $\theta = 1$, $\eta = 0.03$, and $A^0 \equiv 1/30$. Initially there are 1000 criminals and 500 police officers randomly distributed on the 3600 grids. The simulations are run for 1000 time steps.

To simulate this stochastic process, we use the Monte Carlo method. Figure 10 shows the result of the simulations. We observe that the police reduce the attractiveness most effectively when they perform the biased truncated Lévy flight (which together with (47) implies that this patrolling strategy reduces the crime rate most effectively). We also note that a biased random walk strategy is better than an unbiased random walk strategy. These agree with the corresponding results in the one-dimensional space.

4 Discussion

The Truncated Lévy Flight Model generalizes both the Random Walk Model and the Lévy Flight Model. Firstly, the discrete RWM is a special case of the discrete TLFM when $L = 1$. Secondly, as $L \rightarrow \infty$, the continuum limit of TLFM approximates the continuum limit of the LFM.

We then consider the effects of the police patrol assuming that the criminals follow a

truncated Lévy flight. We compare the three patrolling strategies: an unbiased random walk, a biased random walk, and a biased truncated Lévy flight. The results in Section 3.3 show that, with spatially non-uniform initial conditions, the most effective strategy is the biased truncated Lévy flight.

One future direction is to further introduce a mechanism allowing the criminals to leave the system without committing a crime with the appearance of the police as in [13].

5 Appendix

We first show a detailed derivation for (26). Recall that in Section 2.5, we would like to examine the behavior of solutions of the form

$$A(x, t) = \bar{A} + \delta_A e^{\sigma t} e^{ikx}, \quad (51)$$

$$\rho(x, t) = \bar{\rho} + \delta_\rho e^{\sigma t} e^{ikx}. \quad (52)$$

Substituting the solutions into (22), we obtain

$$\begin{aligned} -\eta|k|^2 \delta_A e^{\sigma t} e^{ikx} - \bar{A} + A^0 - \delta_A e^{\sigma t} e^{ikx} + (\bar{A} + \delta_A e^{\sigma t} e^{ikx})(\bar{\rho} + \delta_\rho e^{\sigma t} e^{ikx}) &= \sigma \delta_A e^{\sigma t} e^{ikx}, \\ -\eta|k|^2 \delta_A - \delta_A + \bar{\rho} \delta_A + \bar{A} \delta_\rho + \delta_A \delta_\rho e^{\sigma t} e^{ikx} &= \sigma \delta_A. \end{aligned} \quad (53)$$

We rewrite (53) in the matrix form, ignoring the second order term $\delta_A \delta_\rho e^{\sigma t} e^{ikx}$, and obtain

$$\begin{bmatrix} -\eta|k|^2 - 1 + \bar{\rho} & \bar{A} \end{bmatrix} \begin{bmatrix} \delta_A \\ \delta_\rho \end{bmatrix} = \sigma \delta_A. \quad (54)$$

Similarly for ρ , from (52), we derive the the corresponding matrix equation

$$\begin{bmatrix} -\frac{2\bar{\rho}}{\bar{A}} D|k|^2 - \bar{\rho} & -D|k|^2 - \bar{A} \end{bmatrix} \begin{bmatrix} \delta_A \\ \delta_\rho \end{bmatrix} = \sigma \delta_\rho. \quad (55)$$

Combining (54) and (55), we thus obtain (26).

Now we provide a proof for Theorem 2.1.

Proof of Theorem 2.1. To solve the eigenvalue problem (26), we first rewrite (26) as

$$\begin{bmatrix} -\eta|k|^2 - 1 + \bar{\rho} - \sigma & \bar{A} \\ \frac{2\bar{\rho}}{\bar{A}} D|k|^2 - \bar{\rho} & -D|k|^2 - \bar{A} - \sigma \end{bmatrix} \begin{bmatrix} \delta_A \\ \delta_\rho \end{bmatrix} = 0. \quad (56)$$

By setting the determinant of the square matrix in the left hand side of (56) to be zero, we obtain

$$\sigma^2 - \tau\sigma + \delta = 0, \quad (57)$$

where

$$\tau = -D|k|^2 - \eta|k|^2 - \bar{A} - 1 + \bar{\rho}, \quad (58)$$

$$\delta = D|k|^2(\eta|k|^2 + 1 - 3\bar{\rho}) + \eta|k|^2 \bar{A} + \bar{A}. \quad (59)$$

The equilibrium is stable if and only if both solutions to (57) have negative real parts. Since $\alpha, \beta > 0$, and thus $\bar{A} > 0, 0 < \bar{\rho} < 1$, we observe that $\tau \leq 0$. Therefore, the equilibrium

is stable if and only if $\delta > 0$. We then observe that if $\bar{\rho} < 1/3$, then $\delta > 0$. It follows that the equilibrium is stable when $\bar{\rho} < 1/3$.

Now we consider the case when $\bar{\rho} > 1/3$. Since the equilibrium is unstable if and only if $\delta < 0$, from (59) we rewrite the condition $\delta < 0$ equivalently as

$$\bar{A} < D|k|^2 \left(-1 + \frac{3\bar{\rho}}{\eta|k|^2 + 1} \right), \quad \forall k. \quad (60)$$

Setting $x = \eta|k|^2$, (60) implies

$$\bar{A} < \max_{x \geq 0} \left[D\eta^{-1}x \left(-1 + \frac{3\bar{\rho}}{x+1} \right) \right]. \quad (61)$$

To calculate the right-hand side of (61), we set the derivative of the corresponding function in x equal to zero, and obtain

$$D\eta^{-1}x \frac{-3\bar{\rho}}{(x+1)^2} + D\eta^{-1}(-1 + \frac{3\bar{\rho}}{x+1}) = 0, \quad (62)$$

$$x^2 + 2x + 1 - 3\bar{\rho} = 0.$$

The positive root of (62) is $x = -1 + \sqrt{3\bar{\rho}}$ (recall that $\bar{\rho} > \frac{1}{3}$), which we substitute into (61) and obtain

$$\bar{A} < D\eta^{-1}(-1 + \sqrt{3\bar{\rho}})^2. \quad (63)$$

This together with (60) implies (27) as desired.

To conclude, when $\bar{\rho} < 1/3$, the equilibrium is stable. When $\bar{\rho} > 1/3$, the equilibrium is unstable if and only if (63) is satisfied. \square

6 Acknowledgements

We would like to first thank the Applied and Computational Mathematics REU Program Summer 2015 at UCLA. We would also like to thank the helpful discussions with Professor Theodore Kolokolnikov, Professor Martin Short, Dr. Scott McCalla, Sorathan Chaturapruek, Fei Fang, Albert X. Jiang, and Milind Tambe. Finally, we would like to thank Prof. Adina Ciomaga for providing inspirations for our future work. This work is supported by NSF grant DMS-1045536 and ARO MURI grant W911NF-11-1-0332. L. W. is also partly supported by NSF grant DMS-1620135. C. W. is also partly supported under the NSF grant 0932078000 when she was in residence at the Mathematical Science Research Institute in Berkeley, California, during the Fall, 2015 semester.

References

- [1] N. Bellomo, C. Bianca, and M. S. Mongiovì, “On the modeling of nonlinear interactions in large complex systems,” *Appl. Math. Lett.*, vol. 23, no. 11, pp. 1372–1377, 2010.
- [2] A. Bellouquid and C. Bianca, “Modelling aggregation–fragmentation phenomena from kinetic to macroscopic scales,” *Mathematical and Computer Modelling*, vol. 52, p. 802–813, 2010.
- [3] H. Berestycki and J. Nadal, “Self-organised critical hot spots of criminal activity,” *European Journal of Applied Mathematics*, vol. 21, October 2010.
- [4] D. Brockmann, L. Hufnagel, and T. Geisel, “The scaling laws of human travel,” *Nature*, vol. 439, January 2006.
- [5] T. Budd, “Burglary of domestic dwellings: Findings from the british crime survey,” *Home Office Statistical Bulletin*, vol. 4, 1999.
- [6] S. Chaturapruek, J. Breslau, D. Yazdi, T. Kolokolnikov, and S. G. McCalla, “Crime modeling with Lévy flights,” *SIAM J. Appl. Math.*, vol. 73, no. 4, pp. 1703–1720, 2013.
- [7] A. Chechkin, R. Metzler, J. Klafter, and V. Y. Gonchar, “Introduction to the theory of Lévy flights,” *International Journal of Theoretical and Applied Finance*, vol. 3, 2008.
- [8] J. M. Gau and T. C. Pratt, “Revisiting broken windows theory: Examining the sources of the discriminant validity of perceived disorder and crime,” *Journal of Criminal Justice*, vol. 38, no. 4, pp. 758 – 766, 2010.
- [9] M. C. González, C. A. Hidalgo, and A.-L. Barabási, “Understanding individual human mobility patterns,” *Nature*, vol. 453, June 2008.
- [10] T. Goudon, B. Nkonga, M. Rasclé, and M. Ribot, “Self-organized populations interacting under pursuit-evasion dynamics,” *Phys. D*, vol. 304/305, pp. 1–22, 2015.
- [11] B. E. Harcourt, “Reflecting on the subject: A critique of the social influence conception of deterrence, the broken windows theory, and order-maintenance policing new york style,” *Michigan Law Review*, vol. 97, no. 2, pp. 291–389, 1998.
- [12] A. James, M. J. Plank, and A. M. Edwards, “Assessing Lévy walks as models of animal foraging,” *Journal of the Royal Society, Interface*, vol. 8, September 2011.
- [13] P. A. Jones, P. J. Brantingham, and L. R. Chayes, “Statistical models of criminal behavior: the effects of law enforcement actions,” *Math. Models Methods Appl. Sci.*, vol. 20, no. suppl. 1, pp. 1397–1423, 2010.
- [14] T. Kolokolnikov, J. A. Carrillo, A. Bertozzi, R. Fetecau, and M. Lewis, “Emergent behaviour in multi-particle systems with non-local interactions [Editorial],” *Phys. D*, vol. 260, pp. 1–4, 2013.
- [15] T. Kolokolnikov, M. J. Ward, and J. Wei, “The stability of steady-state hot-spot patterns for a reaction-diffusion model of urban crime,” *Discrete Contin. Dyn. Syst. Ser. B*, vol. 19, no. 5, pp. 1373–1410, 2014.

- [16] P. J. V. Koppen and R. W. J. Jansen, “The road to the robbery: Travel patterns in commercial robberies,” *Br. J. Criminol*, vol. 38, pp. 230–246, 1998.
- [17] D. J. B. Lloyd and H. O’Farrell, “On localised hotspots of an urban crime model,” *Phys. D*, vol. 253, pp. 23–39, 2013.
- [18] R. N. Mantegna and H. E. Stanley, “Stochastic process with ultraslow convergence to a gaussian: The truncated Lévy flight,” *Phys. Rev. Lett.*, vol. 73, pp. 2946–2949, Nov 1994.
- [19] M. C. Mariani and Y. Liu, “Normalized truncated Lévy walks applied to the study of financial indices,” *Physica A: Statistical Mechanics and its Applications*, 2007.
- [20] A. Matacz, “Financial modeling and option theory with the truncated Lévy process,” *International Journal of Theoretical and Applied Finance*, vol. 3, no. 1, 2000.
- [21] L. C. Miranda and R. Riera, “Truncated Lévy walks and an emerging market economic index,” *Physica A: Statistical Mechanics and its Applications*, vol. 297, pp. 509–520, August 2001.
- [22] M. O’Leary, “Modeling criminal distance decay,” *Cityscape: A Journal of Policy Development and Research*, vol. 13, 2011.
- [23] A. B. Pitcher, “Adding police to a mathematical model of burglary,” *European J. Appl. Math.*, vol. 21, no. 4-5, pp. 401–419, 2010.
- [24] N. Rodríguez, “On the global well-posedness theory for a class of PDE models for criminal activity,” *Phys. D*, vol. 260, pp. 191–200, 2013.
- [25] N. Rodriguez and A. Bertozzi, “Local existence and uniqueness of solutions to a PDE model for criminal behavior,” *Math. Models Methods Appl. Sci.*, vol. 20, no. suppl. 1, pp. 1425–1457, 2010.
- [26] M. B. Short, G. O. Mohler, P. J. Brantingham, and G. E. Tita, “Gang rivalry dynamics via coupled point process networks,” *Discrete Contin. Dyn. Syst. Ser. B*, vol. 19, no. 5, pp. 1459–1477, 2014.
- [27] M. B. Short, A. Bertozzi, and P. J. Brantingham, “Nonlinear patterns in urban crime: Hotspots, bifurcations, and suppression,” *SIAM Journal on Applied Dynamical Systems*, vol. 9, no. 2, pp. 462–483, 2010.
- [28] M. B. Short, P. J. Brantingham, A. Bertozzi, and G. E. Tita, “Dissipation and displacement of hotspots in reaction-diffusion models of crime,” *Proc. Nat. Acad. Sci.*, vol. 107, no. 9, pp. 3961–3965, 2010.
- [29] M. B. Short, M. R. D’Orsogna, V. B. Pasour, G. E. Tita, P. J. Brantingham, A. Bertozzi, and L. B. Chayes, “A statistical model of criminal behavior,” *Math. Models Methods Appl. Sci.*, vol. 18, no. suppl., pp. 1249–1267, 2008.
- [30] B. Snook, “Individual differences in distance travelled by serial burglars,” *Journal of Investigative Psychology and Offender Profiling*, vol. 1, 2004.
- [31] H. Spohn, *Large Scale Dynamics of Interacting Particles*, 1991.

- [32] W. H. Tse and M. J. Ward, “Hotspot formation and dynamics for a continuum model of urban crime,” *European J. Appl. Math.*, vol. 27, no. 3, pp. 583–624, 2016.
- [33] F. Vecil, P. Lafitte, and J. Rosado Linares, “A numerical study of attraction/repulsion collective behavior models: 3D particle analyses and 1D kinetic simulations,” *Phys. D*, vol. 260, pp. 127–144, 2013.
- [34] J. R. Zipkin, M. B. Short, and A. Bertozzi, “Cops on the dots in a mathematical model of urban crime and police response,” *Discrete Contin. Dyn. Syst. Ser. B*, vol. 19, no. 5, pp. 1479–1506, 2014.
- [35] A. Zoia, A. Rosso, and M. Kardar, “Fractional laplacian in bounded domains,” *Physical Review*, vol. 76, no. 4, 2007.